

Determination of configurational setting, Ground state Cohesive energies and Harmonic vibration of $Al_8Cu_4Fe_1$, $Al_{27}Cu_{10}Fe_5$ and $Al_{34}Cu_{14}Fe_7$ Icosahedral Clusters Using Fhi-aims Code

S. Mansur¹ and G. Babaji^{1,2}

¹Department of Physics Northwest University Kano

²Department of Physics Bayero University Kano

¹e-mail: msaid@nwu.edu.ng

¹Phone: 08065418754

Abstract

Quasicrystals are material with perfect long-range order, but no three-dimensional translational periodicity. They are typically binary and ternary metallic alloys. Metropolis Monte Carlo rules were used for the study of configurational settings of Mackay icosahedrons clusters with compositions $Al_8Cu_4Fe_1$, $Al_{27}Cu_{10}Fe_5$ and $Al_{34}Cu_{14}Fe_7$. Fhi-aims code was used to study the Total energies, Cohesive energies and Harmonic vibrations of the clusters. It was found that the position of iron and copper were found at vertex 9 and 5 respectively with the transition probability of 1.0022354058 and 0.9301126399 for the first Mackay shells. Also with packing techniques the second and third clusters were formed. $-2.68638.6363293350eV$, $-843443.1972839070eV$ and $-1101611.5411331500eV$ were obtained from the result of geometry optimization of $Al_8Cu_4Fe_1$, $Al_{27}Cu_{10}Fe_5$ and $Al_{34}Cu_{14}Fe_7$ with default Fhi-aims setting. With highest basis size 62, it was found that the total energy of the clusters are $-268652.3373186230 eV$, $-843492.9531392190eV$ and $-1101676.4791576700eV$. For the cohesive energy per atom, it was found that $Al_8Cu_4Fe_1$, $Al_{27}Cu_{10}Fe_5$ and $Al_{34}Cu_{14}Fe_7$ clusters have 2.7eV, 3.1eV and 3.4eV respectively with HOMO-LUMO gaps of 0.41594094 eV, 0.09191654 eV and 0.09281146 eV. However the result of finite difference method for the calculation of infrared spectra for the clusters, shows that; $Al_8Cu_4Fe_1$, spectra have peaks at 94.2, 120.9, 136.5, 157.5, 173, 193.9, 207.6 and 328.9 cm^{-1} , $Al_{27}Cu_{10}Fe_5$ spectra have peaks at 51.3, 66.4, 77.6, 112.2, 161.4, 171.6, 196.9, 231.5, 288.9, 331.8 and 470.1 cm^{-1} and $Al_{34}Cu_{14}Fe_7$ have peak at 38, 64, 99, 135, 162, 232, 239, 286, 313, 335, 460, 496, and 516 cm^{-1} . Also the range of the frequency spectra for the clusters increases as the number of the atoms increases in the cluster. The result of the spectra were compared with the result in the literature.

Keys: Quasicrystals, Icosahedron, Metropolis Monte Carlo, Cohesive Energy, IR-spectrum and Zero-Point-Energy

1.0 Introduction

On the discovery of quasicrystal, the international union of crystallography has redefine the term crystal to mean “any solid having essentially discrete diffraction diagram”, thereby shortening the essential attribute of crystallinity from position space to Fourier space [1]. Thus it is possible to obtain an infinitely extended crystal structure by aligning building blocks called unit-cell until the space is filled up. In 1985, Dan shechtman, Blech, Gratias and Cahn discover quasi-crystals [2] are

well ordered but aperiodic intermetallics. These are typically binary and ternary metallic alloys often containing (60–70) percent aluminum which exhibit unusual physical properties, such as low friction, low adhesion, high hardness and high wear resistance[3].

Quasicrystals present a unique structural features to surface science that is quite unusual because; they are neither periodically ordered like crystals nor disordered like amorphous solid. They have a well define discrete group symmetry like crystal which are not compatible with allowed crystallographic symmetry such as 5, 8, 10 or 12-fold symmetry. Also strange about quasicrystals is that many of their mechanical-physical properties are quite unusual by the standard of common metals. Some of these properties are surface related [3].

Clusters are usually used to describe aggregates of atoms that are too large to be referred to as molecules and too small to resemble small pieces of crystals. Clusters generally do not have the same structure or atomic arrangement as a bulk solid[4]. Clusters may be classified as metallic or nonmetallic according to the atoms they are made of in general some metallic character persists from small clusters to bulk matter of the same composition. Atoms are easily classified as metallic, nonmetallic or semiconducting purely in terms of their ionization potentials [5]. Developments in nanoscale science enable scientists to atomically engineer and characterize clusters of any size and composition. The importance of these developments lies in the fact that clusters offered a novel class of materials with electronic, catalytic and magnetic properties that are different from the bulk.

There are many work done in the quasicrystal among which include the work of Quiquandon [6] on quasicrystal and approximant structures in Al-Cu-Fe, suggested that icosahedral phase both via systematic introduction of atomic jumps preserving most of the atomic local environments and via long-range atomic diffusion. Feridoun [3], proposed that study of quasicrystal is very important especially for the surface scientists because of some strange properties observed which are not observed in metals such as low surface energies and coefficients of friction, good oxidation and corrosion resistance and high hardness. Also they are available, low-cost and non-toxic". Jurgen Hafner [7], reported on the nucleation of Pb layers on five-fold surface of icosahedral known as *starfish*. Keisuke [8] reported the different models in describing quasicrystal cluster starting from the work of Shechtman [2] Stephens [9] and Elser [10] and they suggested that clusters join together under some constraint to maintain orientational order. Onoda [11] reported the discovery of an algorithm for building a perfect 2D Penrose tiling by "local" rules, which is apparently

inconsistent with Penrose's theorem, which states that Penrose tiling cannot be built by local rules. Jeong [12] extended Onoda's work and developed an algorithm for the growth of a perfect 3D decagonal quasicrystal that consists of a periodic stacking of 2D Penrose tilings. Olami [13] proposed a growth model for a pentagonal quasicrystalline tiling by local rules, generating highly ordered quasicrystals with limited disorder in a tile arrangement.

However, information about the vibrational spectra of quasicrystals is very poor and mainly based on the result of experimental investigations. There have been only three theoretical studies devoted to the analysis of vibrational spectra of quasicrystals. In one of them, the general properties of the vibrational behaviour of quasicrystalline objects were discussed on 1D quasiperiodic chain [14]. The second study was on vibrational spectra and some thermodynamic properties of a number of 2D quasicrystals of octagonal and decagonal types [15]. The third was on the vibrational spectra of an icosahedral quasicrystal [16].

Quasicrystal was identified as non-toxic, low cost, corrosion resistance and good oxidation, demand for substituting this alloy requires further investigating of this material especially in our locality, as Nigeria being a country with abundant mineral resources. The work aimed at constructing the icosahedral clusters using Mackay model of first shell. Metropolis Monte Carlo approach was used to determine the best configuration for the interested cluster. Geometry optimization was used for each shell. Total energies and cohesive energy per atom were calculated at different basis size. Harmonic vibration of each cluster using finite difference for the IR spectra was calculated using FHI-aims [17] which uses Density Functional Theory (DFT) as a main production technique to determine electronic and structural properties of a cluster with icosahedral composition AlCuFe.

2.0 Theoretical Background

2.1 Calculation of the vibration and vibrational free energy of clusters

The dynamic behavior of a cluster is described by set of coordinate [18];

$$r_1, r_2, \dots, r_N \quad (1)$$

which are treated as time dependent variable. The particles within the cluster are assumed to interact via binary potential v_p which depends only on their relative position;

$$v_p(r_i, r_j) = v_p(r_i - r_j) \quad (2)$$

The total potential energy of the cluster, v_p is assumed to be given by the summation of binary interactions over all the pair particles in the cluster;

$$V_p(r_1 \dots r_N) = \sum_{i>j} v_p(|r_i - r_j|) \quad (3)$$

where the dependence of the potential energy on the cluster configuration has been emphasized. The configuration of a cluster which minimizes the potential energy function can be denoted by the set of coordinates

$$r_1^o, r_2^o, \dots, r_N^o \quad (4)$$

denoted by mean static position of N particle within the cluster.

Assuming that;

$$u_i = r_i - r_j^o; |u_i| \ll |r_i^o - r_j^o| \quad \forall i, j \in 1, \dots, N \quad (5)$$

the displacement of particles from their equilibrium position are small, one can expand the total potential energy of the cluster in Tylor series up to the second order as;

$$V_p(r_1 \dots r_N) = v_p(r_i^o - r_j^o) + 1/2 \sum_{i,j} \sum_{\alpha,\beta} U_i^\alpha U_j^\beta \frac{d^2 v_p}{dr_i^\alpha dr_j^\beta} \quad (6)$$

where α and β denote the Cartesian component of (X,Y and Z) of vectors. The first derivatives of v_p with respect to atom coordinate are assumed to vanish that is, the cluster is assume to be minimum potential energy configuration and this is well known as harmonic approximation and it serves as starting point for calculation of cluster normal mode of vibration (i.e a set of linear combination of (u_i, \dots, u_N) variables or eigenmodes each of which correspond to a vibration of the system with single frequency). The Hamiltonian of the problem when written in terms of normal mode coordinates represent a set of independent harmonic oscillation whose both quantum and classical dynamic are well known. There are $3N - 6$ such oscillations with characteristic frequency ω_p with $p = 1, \dots, 3N - 6$. Six degree of freedom that does not represent vibrations is the three rotations and three translation of the whole system. Once a set of

eigenfrequencies are calculated one can proceed to calculate the Helmholtz free energy of the cluster F which is given as;

$$F = -K_B T \ln Z \quad (7)$$

where K_B is Boltzmann constant T is temperature and Z is quantum partition function of the system of 3N-6 independent oscillators. Equation 7 can be expressed in term of eigenmodes frequencies as;

$$F = V_p^o + \sum_{p=1}^{3N-6} \frac{h\omega_p}{2} + K_B T \sum_{p=1}^{3N-6} \ln \left[1 - \exp \left(-\frac{h\omega_p}{K_B T} \right) \right] \quad (8)$$

where

$$V_p^o = v_p [r_1^o, \dots, r_N^o] \quad (9)$$

The above equation is the minimum of classical potential energy of the cluster (ground state energy). The sum of the first two terms in equation 8 represents the quantum ground state of the cluster, E_o calculated in the harmonic approximation. At constant temperature, the state which represents the thermodynamical equilibrium of the system is the one which minimizes the Helmholtz free energy. (NB even at zero temperature, the cluster free energy has a quantum zero-point energy contribution). Thus even at zero temperature the thermodynamical equilibrium state of the cluster need not to be the same as the state which minimizes the classical potential energy of the cluster [18].

2.2 Monte Carlo

Monte Carlo method is a common name for a wide variety of stochastic techniques. These techniques are based on the use of random numbers and probability statistics to investigate problems in areas as diverse as economics, material science, nuclear physics and flow of traffic. In general, to call something a "Monte Carlo" method, all you need to do is use random numbers to examine your problem [19].

2.2.1 Metropolis Monte Carlo

Metropolis Monte Carlo is a method that generates configuration according to the desired statistical mechanics distribution. The method is used to study equilibrium properties of the

system, its the step-by-step method for finding the configuration according to the iterative procedure. For an initial configuration (n_i : old), generate a new configuration(n_{i+1} : new) by randomly changing the positions of atoms or groups of atoms (called "MC move" and are performed on dihedral angles in internal coordinates) and evaluate the potential energy or total energy of the new configuration $E(n)$, the new configuration is accepted or rejected by computing the energy differences as [19].

$$\Delta E = E(n_{i+1}) - E(n_i) \quad (10)$$

and evaluate transition probability

$$v(n_i, n_{i+1}) = \frac{P_B(n_{i+1})}{P_B(n_i)} = \min[1, e^{-\Delta E}] \quad (11)$$

$\Delta E \leq 0$: always accept new configuration.

$\Delta E > 0$: reject the configuration

repeat the the for another sampling untill the right configuration is found.

2.2 Density Functional Theory

Density Functional Theory (DFT) is a quantum mechanical technique used in physics and chemistry to investigate the structural and electronic properties of many body systems. DFT has proved to be highly successful in describing structural and electronic properties in a vast class of materials, ranging from atoms, molecules, clusters and bulk to sample crystals and complex extended systems [20]. DFT has become a substitute of traditional method of describing electronic structure such as Hartree-fock theory and its descendents(i.e DFT replace the many-body electronic wavefunction with electronic density as the basis quantity).

Hohenberg and Khon [21] demonstrated the ground-state wavefunction in the form of density. For many-electron Hamiltonian

$$H = T + U + V \quad (12)$$

with ground state wavefunction Ψ , the kinetic energy T, electron-electro interaction U and external potential V. The charge density $\eta(r)$ as;

$$\eta(r) = \int |\Psi(r_1, r_2, r_3, \dots, r_N)|^2 dr_1 \dots dr_N \quad (13)$$

considering a different Hamiltonian which the external potential do not differ with V such that $V - V' \neq \text{constant}$, then the total energy is

$$E = \langle \Psi' | H' | \Psi' \rangle < \langle \Psi | H' | \Psi \rangle = \langle \Psi | H + V' - V | \Psi \rangle \quad (14)$$

that is

$$E' < E + \int (V(r) - V'(r))\eta(r)dr \quad (15)$$

The total energy

$$E[\eta(r)] = (\Psi | T + U + V | \Psi) = (\Psi | T + U | \Psi) + (\Psi | V | \Psi) = F[\eta(r)] + \int \eta(r)V(r)dr \quad (16)$$

Thus DFT reduces the N-body problem to the determination of a 3-dimensional function $\eta(r)$ which minimizes a functional $E[\eta(r)]$.

Khon and Sham [22] reformulated the problem in a more familiar form and opened the way to practical applications of DFT [23-25]. For a system of interacting and non-interacting body have the same ground state charge density $\eta(r)$ and thus is the sum over one-electron orbital Ψ_i [24, 26]:

$$\eta(r) = 2\sum |\Psi_i(r)|^2 \quad (17)$$

where i runs from 1 to $\frac{N}{2}$, the value of Ψ_i is the solution of the schrodinger equation as;

$$\left(\frac{\hbar^2}{2m}\nabla^2 + V_{KS}(r)\right)\Psi_i(r) = \epsilon_i \Psi_i(r) \quad (18)$$

the equation is solve using variational property of energy. For an arbitrary variation of the $\Psi_i(r)$, the variation of E must vanish. This translates into the condition that the functional derivative with respect to the Ψ_i of the constrained functional.

$$E' = E - \sum_{ij} \lambda_{ij} \left(\int \Psi_i^*(r) \Psi_j(r) dr - \delta_{ij} \right) \quad (19)$$

where the lagrange multipliers, λ_{ij} must vanish [27]:

$$\frac{\partial E'}{\partial \Psi_i^*(r)} = \frac{\partial E'}{\partial \Psi_i(r)} = 0 \quad (20)$$

the fluctuation energy is written as

$$E = T[\eta(r)] + E_H[\eta(r)] + E_{xc}[\eta(r)] + \int \eta(r)V(r)dr \quad (21)$$

The first term is the kinetic energy of non-interacting electrons, the second term (Hartree energy) is the electrostatic interaction between clouds of charge, the third term is the exchange-correlation energy and the fourth term is the external potential. Hence equation (18) can be written as;

$$\left(\frac{\hbar^2}{2m}\nabla^2 + V_H(r) + V_{xc}[\eta(r)] + V(r)\right)\Psi_i(r) = \sum_j \lambda_{ij} \Psi_j(r) \quad (22)$$

2.3 Exchange correlation Functional

2.3.1 Generalized Gradient Approximation Functional

In generalized gradient approximation (GGA), the exchange-correlation potential is treated as a function of both electron density as well as the gradient of the density. The exchange-correlation functional in GGA has the form;

$$\delta E_{xc}[\eta] = \sum_{\sigma} \int dr \left[\varepsilon_{xc} + \eta \frac{\partial \varepsilon_{xc}}{\partial \eta^{\sigma}} + \eta \frac{\partial \varepsilon_{xc}}{\partial \nabla \eta^{\sigma}} \right]_{r,\sigma} \delta \eta(r, \sigma) \quad (23)$$

where the term in the bracket is the exchange -correlation potential as;

$$\delta V_{xc}^{\sigma}[\eta] = \left[\varepsilon_{xc} + \eta \frac{\partial \varepsilon_{xc}}{\partial \eta^{\sigma}} + \eta \frac{\partial \varepsilon_{xc}}{\partial \nabla \eta^{\sigma}} \right]_{r,\sigma} \quad (24)$$

2.3.2 Generalized Gradient Approximation + Vander Waal (GGA+vdW)

Vander Waal forces are the residual attractive or repulsive forces between molecules or clusters that do not arise from a covalent bond or electrostatic interactions of ion or ionic group with one another.

Nowadays it is well known that most popular exchange functionals generally show unsatisfactory performance for vdW forces, which inherently arise due to nonlocal correlations [28]. In order to test if the lack of vdW forces is indeed responsible for the underestimation in the two body interaction we use a simple $C_6 R^{-6}$ correction for the DFT total energies. The $C_6 R^{-6}$ correction method was early proposed for correcting HF calculation [29] and specifically applied to DFT [30-32]. certainly the $C_6 R^{-6}$ pairwise scheme is a simple one for incorporation dispersion interaction into DFT calculations in contrast to other approaches. With this approach the pairwise vdW interaction (E_{dis}) is calculated by

$$E_{disp} = -\sum_{j>i} f_{damp}(R_{ij}, R_{ij}^o) C_{6ij} R_{ij}^{-6} \quad (25)$$

where C_{6ij} are the dispersion coefficients for an atom pair ij, R_{ij} is the interatomic distances,

R_{ij}^o is the sum of equilibrium vdW distances for the pair and damping function. The damping function is needed to avoid the divergence of the R^{-6} term at short distances and reduces the effect of the correction on covalent bonds [28].

3 Methodology

Fhi-aims(Fritz Haber Institute ab-initio molecular simulation) is a computer program package for computational material science based on quantum-mechanical first principles. The main production method is density functional theory(DFT) to compute the total energy and derived quantities of molecular, cluster or solid condensed matter in its electronic ground state. In addition FHI-aims allows to describe electronic single quasiparticle excitations in molecules using different self-energy formalisms, and wave-function based molecular total energy calculation based on Hartree-Fock and manybody perturbation theory [33].

The focus here is on density functional theory(DFT) in the local and semi-local (generalized gradient) approximations but an extension on hybrid functional, Hartree-Fock theory, and MP2/GW electron self-energies for local energies and excited states is possible with the same underlying algorithms. An all electron/full-potential treatment that is both computationally efficient and accurate is achieved for periodic and cluster geometries on equal footing, including relaxation and ab initio molecular dynamics [34]. The construction of transferable, hierarchical basis set is demonstrated, allowing the calculation to range from qualitative tight-binding like accuracy to meV-level total energy convergence with basis set. Together with scalar-relativistic treatment, the basis sets provide access to all elements from light to heavy. Both low-communication parallelization of all real-space grid based algorithms and a scalapack-based, customized handling of the linear algebra for all matrix operations are possible, guaranteeing efficient scaling (CPU time and memory) up to massively parallel computer system with thousand of CPUs [34].

3.1 Building of Cluster

The convex regular icosahedron is the more common and is usually referred to simply as the regular icosahedron, one of the five regular Platonic solids, and is represented by its Schläfli symbol [3, 5], containing 20 triangular faces, with 5 faces meeting around each vertex.

The geometry (i.e coordinate of the vertices) of the first Mackay shell Icosahedron was obtained from [35]. A lattice constant of 2.83\AA was applied and the atoms were randomly assigned to the

vertices . The Fhi-aims Metropolis monte carlo (equation 10 and 11) was implimented to find the most stable monomer(see table table 1 and 2 for Monte Carlo moves of Copper and iron in first mackay shell). The original coordinates and the and most stable monomer are given in the appendix 1 table A-C. However in case of the second Mackay shell three first shell were packed and three additional atoms were added. And in the case of third shell one additional first Mackay shell was addedto the second. For second and third Mackay shell each time Fhi-aims Metropolis monte carlo was applied for the most stable monomer as shown in figure 1.

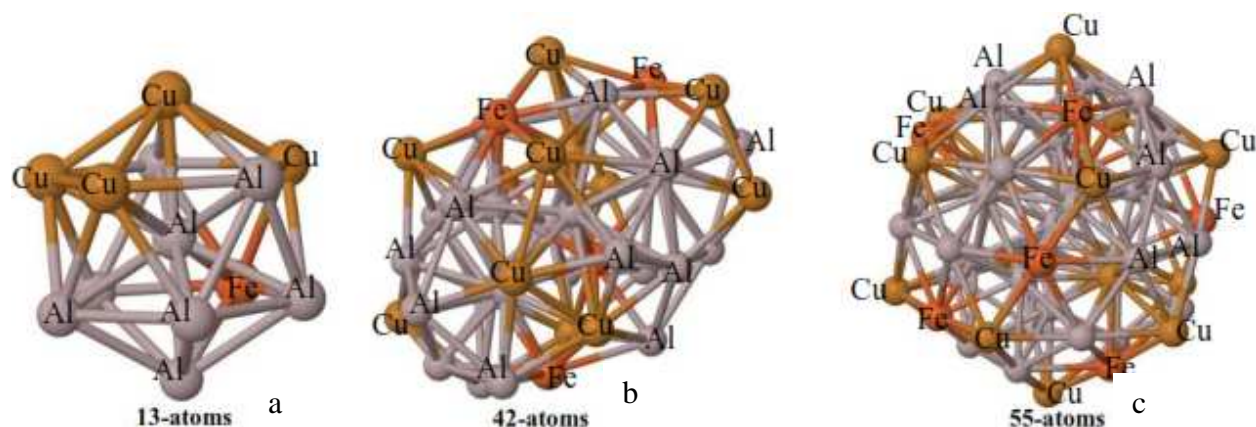


Figure 1: Icosahedral Clusters (a) $Al_8Cu_4Fe_1$ (b) $Al_{27}Cu_{10}Fe_5$ (c) $Al_{34}Cu_{14}Fe_7$ an image produce using Jmol

3.2 Geometry Optimization

The parameters exchange functional (*pbe+vdW*), spin (*collinear*),*default_initial_moment(hund)* and *zero-Order-regular-approximation*were kept fixed while the parameters *Occupation-type-gaussian*, *charge-mix-paramsc_accuracy_rho*, *sc_accuracy_etot*, *sc_accuracy_eev*, *sc_accuracy_forces* and *relax_geometry_Bfgs* were optimized. The above procedure was repeated for each cluster and each time, total energy and total cpu time were recorded as shown in table 3-5. Another optimizations was run for the optimize parameters for each cluster

3.3 Effect of Basis Size

After obtaining the converge geometry, the calculation of basis size was employed for the optimized structure. Each element has different basis set. For aluminum there are sixteen basis size of which four are minimal basis, eight *tier₁* twelve *tier₂* and sixteen *tier₃*, for Copper ther are twenty one basis size of which 6 are minimal, 11 *tier₁*, 16 *tier₂* and 21 *tier₃* and lastly Iron there

are twenty five basis size of which 6 minimal 11 $tier_1$, 18 $tier_2$ and 25 $tier_3$. The procedure were repeated for metallic alloy and for each time the total energy was recorded.

3.4 Calculation of Cohesive Energy

The free atom total energy of Aluminum, Copper and Iron were obtained using Fhi-aims. The cohesive energy per atom was obtained from equation 26

$$E_{cohesive} = \frac{1}{N} [E_{total} - \Sigma(aE_{al} + bE_{cu} + cE_{fe})] \quad (26)$$

where $N = a + b + c$, E_{total} = total energy of the cluster, E_{al} , E_{cu} and E_{fe} = toatal energy of free atom of aluminum, copper and Iron respectively and a, b and c are number of aluminum, copper and iron in the cluster.

3.5 Harmonic Vibration

with the optimized geometry, finite different calculation was employed using fhi-aims. from the **control.in** file; *relax_geometry_bfgs 1.0E-5*, *default_initial_moment (hund)* and *zora* were commented and the vibration runs. for each cluster the above procedure was repeated and the files contains the informations for IR, Normal mode, zero point energy was further analized using molden molecular viewer.

4 Result

4.1 Metropolis Motecarlo Configuration of First Mackay Shell

Table 1: Configuration Setting for Iron using Metropolis Monte Carlo rule

position	TotalEnergy (eV)	Time (s)	No.Scc	Relax. steps	ΔE (eV)	$v(O_i, n_{i+1})$
position_1	-268650.196909506	2179.292	8702	56		
position_2	-268650.215575727	2102.091	9098	58	-0.018666221	1.018841524
position_3	-268650.486788745	2150.226	8423	49	-0.289879239	1.3362661094
position_4	-268650.304931134	1692.986	7040	50	-0.108021628	1.1140718403
position_5	-268649.994485883	2151.806	8568	63	0.202423623	0.816748861
position_6	-268650.128848849	1087.228	4796	45	0.068060657	0.9342038058
position_7	-268650.083995341	2752.872	10973	72	0.112914165	0.893227327
position_8	-268650.501272248	2904.442	12744	91	-0.304362742	1.3557607583
position_9	-268650.199142417	2000.717	8324	55	-0.002232911	1.0022354058

position_10	-268650.129972496	1377.55	6088	49	0.06693701	0.9352541112
position_11	-268647.407594884	166.622	1292	1	2.789314622	0.0614633251
position_12	-268650.344105536	2466.03	10356	66	-0.14719603	1.1585810574
position_13	no	no	no	no		

Table 2: Configuration Setting for Copper using Metropolis Monte Carlo rule

position	Total Energy (eV)	Time (s)	No. Scs	Relax. steps	ΔE (eV)	$v(O_i, n_{i+1})$
Position_1	-268650.544046307	4947.617	19858	106		
Position_2	-268649.946380131	3443.839	14221	83	0.597666176	1.8178712542
Position_3	-268650.198677982	1752.186	7319	53	0.345368325	1.4125100866
Position_4	-268650.354436762	3504.843	14004	67	0.189609545	1.2087775323
Position_5	-268650.616495889	2124.901	8865	54	-0.072449582	0.9301126399
Position_6	-268650.219427800	3104.062	11923	68	0.324618507	1.3835027487
Position_7	-268650.215901248	2140.718	9409	60	0.328145059	1.3883903562

4.2 Optimization of Key Parameters

Table 3: Optimized Parameters of $Al_8Cu_4Fe_1$ of the First Mackay Shell of Icosahedron using pbe+vdW

Parameter	Optimized value	Total Energy(eV)	Time(s)
occupation_type Gaussian	0.09	-268652.013937163	5585.381
charge_mix_param	0.03	-268651.964975413	1875.837
sc_accuracy_rho	0.0001	-268651.964975705	5670.222
sc_accuracy_eev	0.0000001	-268651.964975411	3902.412
sc_accuracy_etot	0.0001	-268651.964975705	5669.814
sc_accuracy_forces	0.00001	-268651.964975705	5643.033
relax_geometry	0.0000001	-268651.964975566	18716.622

Table 4: Optimized Parameters of $Al_{27}Cu_{10}Fe_5$ of the Second Mackay Shell of Icosahedron using pbe+vdW

Parameter	Optimized value	Total Energy(eV)	Time(s)
occupation_type Gaussian	0.05	-843492.11738935	530.257
charge_mix_param	0.001	-843490.332856425	3872.506
sc_accuracy_rho	0.0001	-843490.332836115	525.857
sc_accuracy_eev	0.00001	-843490.332836115	517.3
sc_accuracy_etot	0.00001	-843490.332836115	517.656
sc_accuracy_forces	0.0001	-843490.332836115	522.025
relax_geometry	0.000001	-843494.332856425	4872.506

Table 5: Optimized Parameters of $Al_{34}Cu_{14}Fe_7$ of the Third Mackay Shell of Icosahedron using pbe+vdW

Parameter	Optimized value	Total Energy(eV)	Time(s)
occupation_type Gaussian	0.1	-1101678.0197619	9120.53
charge_mix_param	0.003	-1101675.87714962	1016.232
sc_accuracy_rho	0.000001	-1101677.3049569	8744.018
sc_accuracy_eev	0.00001	-1101677.3049569	8090.038
sc_accuracy_etot	0.0001	-1101677.76752486	8744.018
sc_accuracy_forces	0.0001	-1101677.3049569	8090.038
relax_geometry	0.00001	-1101678.0197619	9120.53

4.3 Calculation of Basis Size of the Clusters

Table 6: Single Point Calculation for Different Basis Size of the Clusters

Basis size	$Energy_{13-atoms}$	$Energy_{42-atoms}$	$Energy_{55-atoms}$
16	-268638.6363293350	-843443.1972839070	-1101611.5411331500
30	-268652.0139371770	-843492.1173992060	-1101675.4146177400
46	-268652.2959147540	-843492.8531392190	-1101676.3791576700
62	-268652.3373186230	-843492.9531392190	-1101676.4791576700

4.4 Evolution of Cohesive Energy with increase in number of cluster of AlCuFe quasicrystal

Table 7: cohesive energy table for the clusters using pbe+vdW exchange functional

Composition	Total Energy(eV)	Exchange	Cohesive Energy(eV)
$Al_8Cu_4Fe_1$	-268652.3373186230	Pbe+vdW	2.7
$Al_{27}Cu_{10}Fe_5$	-843492.9531392190	Pbe+vdW	3.1
$Al_{34}Cu_{14}Fe_7$	-1101676.4791576700	Pbe+vdW	3.4

4.5 Evolution of Ir-Spectra with increase in number of atoms

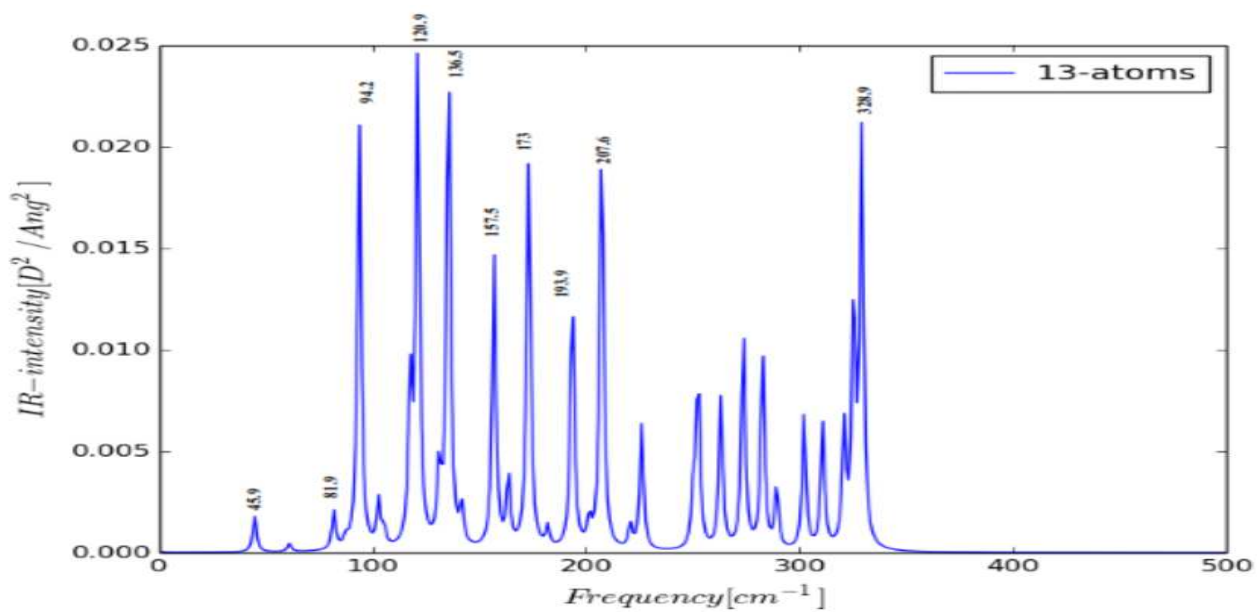


Figure 3: Graph of Ir-Spectra vs frequency of $Al_8Cu_4Fe_1$ Icosahedron Cluster

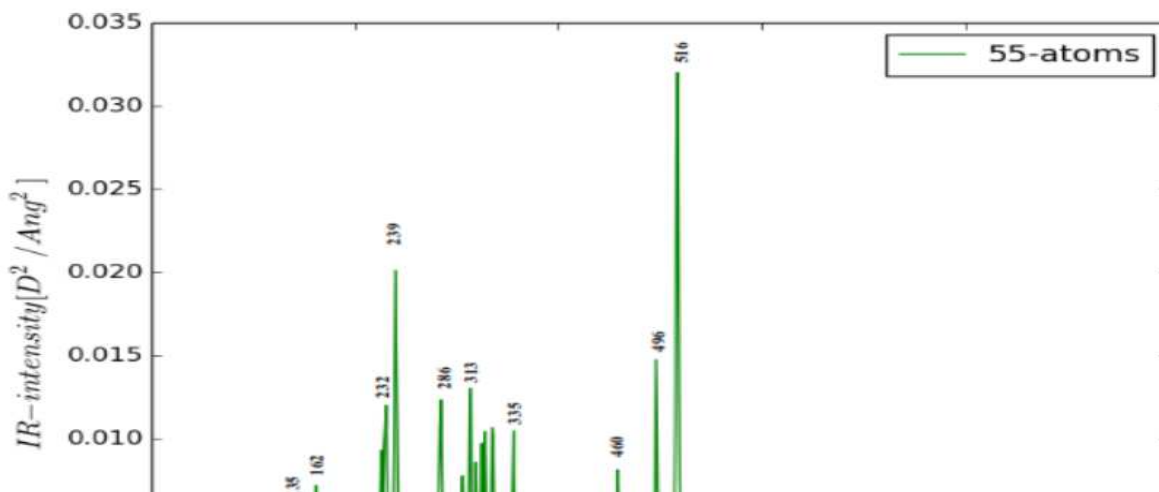
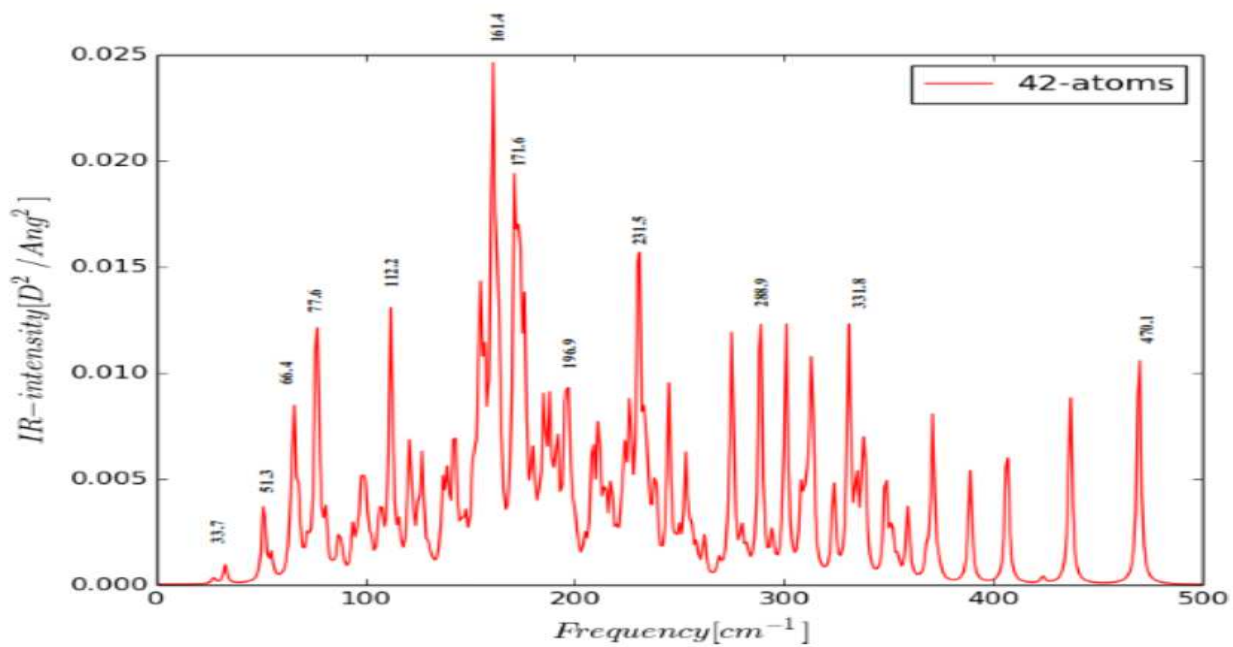


Figure 4: Graph of Ir-Spectra vs frequency of $Al_{27}Cu_{10}Fe_5$ Icosahedron Cluster



Figure 5: Graph of Ir-Spectra vs frequency of $Al_{34}Cu_{14}Fe_7$ Icosahedral Cluster

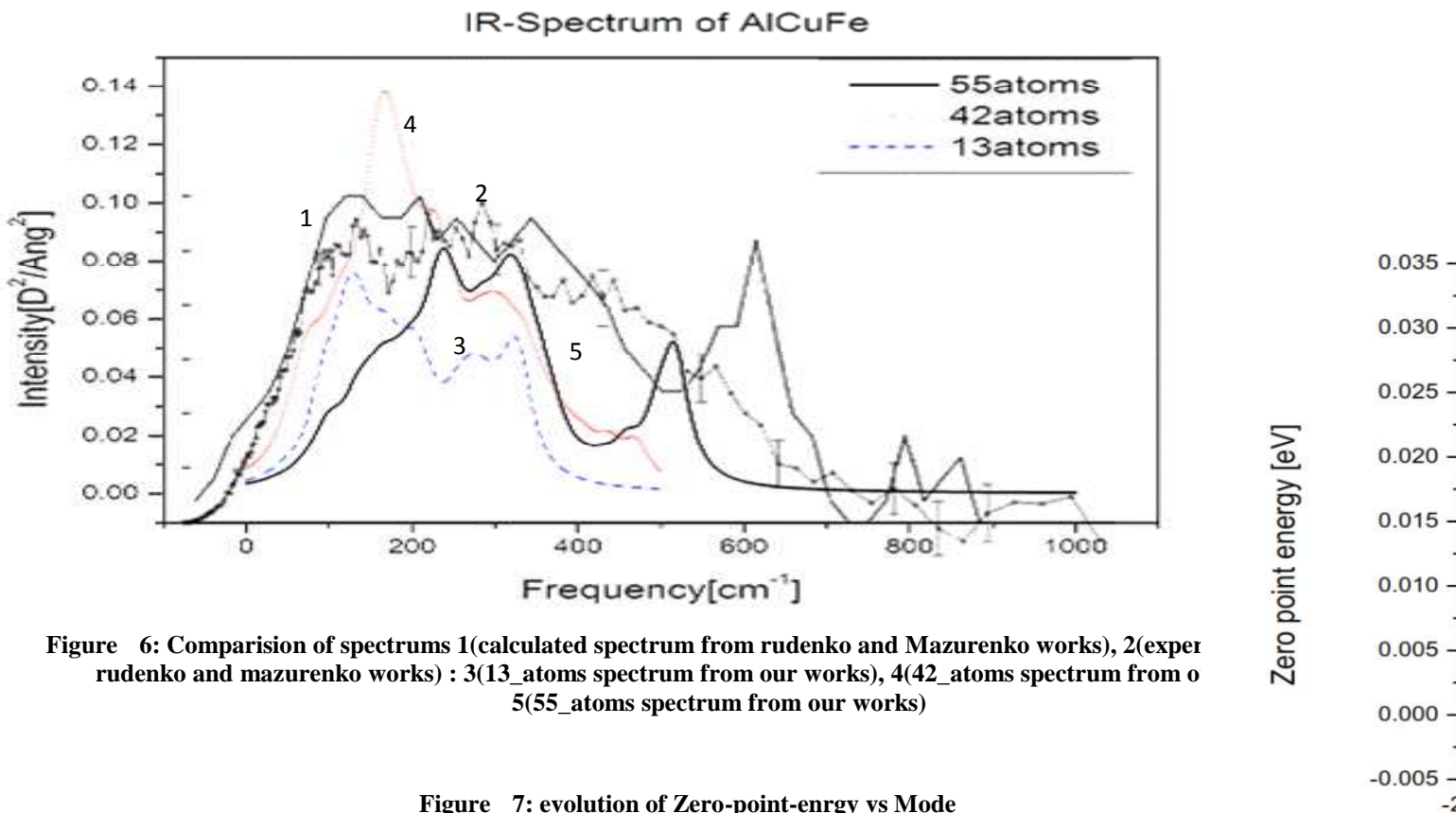


Figure 6: Comparison of spectrums 1(calculated spectrum from rudenko and Mazurenko works), 2(exper rudenko and mazurenko works) : 3(13_atoms spectrum from our works), 4(42_atoms spectrum from o 5(55_atoms spectrum from our works)

Figure 7: evolution of Zero-point-energy vs Mode
 Figure 7: evolution of Zero-point-enrgy vs Mode

Mode

4.6 Discussion

Table 1 and 2 showed the result of the configuration setting using Metropolis Monte Carlo rule equation 10 and 11. In Table1, it was observed that the best position of the iron element in structure is at *position₉*, and in table2 the best position of copper was at *poision₅* for each table, column five shows the probability of finding the element in the position. Packing of $Al_8Cu_4Fe_1$, was used for bulding of $Al_{27}Cu_{10}Fe_5$ and $Al_{34}Cu_{14}Fe_7$ clusters. three atoms was added for the bulding of $Al_{27}Cu_{10}Fe_5$.

Table 3,4 and 5 shows the results for number of pre-selection of values for optimization of each cluster with the exchange functional GGA+vdW (*pbe+vdw-correction-hirshfeld*). It was observed that the optimized values for each cluster is different due to the different composition of the cluster and the result shows that the higher the number of atoms in the cluster the lower the total energy. From the single point calculation in Table 6, it was depicted that lowest energy is

found by increasing the number of basis size.

Table 7 shows the evolution effect of cohesive energy of the cluster and hence cohesive energy increases as the number of atoms increases in the cluster. However the structure with 55 atoms have the most stable surface and its icosahedral structure is maintained. Highest Occupied Molecular Orbital to Lowest Unoccupied Molecular Orbital (HOMO-LUMO) gap is another sensitive quantity used to prove the stability of the structure, this energy gap depends on the material. for $Al_8Cu_4Fe_1$, $Al_{27}Cu_{10}Fe_5$ and $Al_{34}Cu_{14}Fe_{10}$ the HOMO-LUMO gap are 0.41594094 eV, 0.09191654 eV and 0.09281146 eV respectively, this shows that HOMO-LUMO gap decreases with increase in number of atoms in the cluster.

Figure. 3, 4 and 5 showed the Infrared (IR) spectrum of clusters $Al_8Cu_4Fe_1$, $Al_{27}Cu_{10}Fe_5$ and $Al_{34}Cu_{14}Fe_{10}$ respectively. it was observed that peaks are appears at different positions; $Al_8Cu_4Fe_1$, spectra have peaks at 94.2, 120.9, 136.5, 157.5, 173, 193.9, 207.6 and 328.9 cm^{-1} , $Al_{27}Cu_{10}Fe_5$ spectra have peaks at 51.3, 66.4, 77.6, 112.2, 161.4, 171.6, 196.9, 231.5, 288.9, 331.8 and 470.1 cm^{-1} and $Al_{34}Cu_{14}Fe_7$ have peak at 38, 64, 99, 135, 162, 232, 239, 286, 313, 335, 460, 496, and 516 cm^{-1} . Also the range of the frequency spectrum for the clusters increases as the number of the atoms increases in the cluster. Figure 6 shows the comparison of our work with that of Rudenko and similar behaviour are observed [16]. on the other hand the zero point energies of the clusters are 0.39179912 eV, 1.49361724 eV, and 2.06408161 eV respectively and it shows that the zero point energy is depends on the number of atoms in the cluster (see Fig.6).

However, position of pure ir spectrum of Al, Cu and Fe were reported in our last seminar and hence the peaks appear at positions; For $Al_8Cu_4Fe_1$ Aluminum 136 cm^{-1} , copper ,94 cm^{-1} , 157 cm^{-1} and 207 cm^{-1} . For $Al_{27}Cu_{10}Fe_5$; copper 112 cm^{-1} , 231 cm^{-1} and 288 cm^{-1} , Fe 161 cm^{-1} and 331 cm^{-1} and Al 171 cm^{-1} . For $Al_{34}Cu_{14}Fe_{10}$; copper 135 cm^{-1} , 232 cm^{-1} , 239 cm^{-1} , Fe 99 cm^{-1} , 162 cm^{-1} and 335 cm^{-1} and Al 376 cm^{-1} and the remaining were due to the cluster formation in each cluster.

5.0 Conclusion

In this work, configurations setting, ground state cohesive energy and harmonic vibration of $Al_8Cu_4Fe_1$, $Al_{27}Cu_{10}Fe_5$ and $Al_{34}Cu_{14}Fe_{10}$ cluster were reported. Phi-aims Metropolis Monte Carlo rule was used for constructing icosahedral clusters. Geometry optimization was used on each cluster after optimizing the parameters. Effect of the basis size on each cluster was also

reported. evolution of cohesive energies with number on atoms was plotted. IR spectrum of each composition was calculated using finite difference, the graph of intensity against frequency was presented. Homo-Lomo energy gap, zero point energy results were also presented for each cluster.

REFERENCE

- [1] Said, M., Babaji, G. and Gidado, A.S. (2014). The effect of shape of atomic potential on diffraction pattern of one dimensional quasicrystal material. *Bajopas, Volume 7*, 62-71.
- [2] Shechtman, D., Btech, I., Gratias, D and Cahn, J. (1985). Metallic phase with long -Range orientational order and NO Translational Symmetry. *Physical letter, Volume 53b*, 19511953.
- [3] Feridoun, S., Mohammad, H. T., Safdar, H., Babak, J. and Parisa, T.A. . (2012). Quasicrystals. *open journal of physical chemistry*, 7-14.
- [4] Viktor Balema.,(2007). Advance Metals and Alloys. *Material Matters 2(4) Aldrich chemistry*.
- [5] Nusret, D., Mehmet, F. F. and Isik, O. (2012) Ni55 nanocluster: density functional theory study of binding energy of nickel and ethylene adsorption. *Turk. J. chem.* **36**55-67.
- [6] Quiquandon, M., Quivy, A., Devaud, J., Faudot, F., Lefebvre, S., Bessiere, M., and Calvayrac, Y. (1996). Quasicrystal and approximant structure in Al-Cu-Fe system. *J.Phys.:Condens. Matter*, 2487-2512.
- [7] Jurgen Hafner, (2010) Ab-initio density functional calculation in materials science: from quasicrystals overmicroporous catalyts to spintrous. *Journal of physics; condense matter vol 22 no. 38*
- [8] Keisuke, N., Tomoaki, I., Kazue, N. and Keiichi, E. (2015) Experimental observation of quasicrystal growth. *Physs.Rev. let 115; 075601*.
- [9] Stephens, P.W., M., Jaric, M. and Gratias D. (1989). Apeiodicity, and Order 3. *Academic Press, Boston,, 37–104*.
- [10] Elser, E., Jaric, M. and Gratias, D. . (1989). in Apeiodicity, and Order 3. *Academic Press, Boston,, 105–136*.
- [11] Onoda, G.Y., Steinhardt, P.J., DiVincenzo, D.P. and Socolar, J. E. S. (1988). *Phys. Rev. Lett.*, 2653.
- [12] Jeong, H. (2007). *Phys. Rev. Lett.*, 98, 135501.
- [13] Olami, Z. (1991). *Europhys. Lett.*, 16, 361.

- [14] Janssen, T. (2002). in Quasicrystal: An Introduction to Structure, Physical Properties and Application. (J. S. Suck, Ed.) *Springer Ser. Mater.Sci*, 55, 423.
- [15] Elhor, H. (2003). Dissertation. *Tech. Univ. Chemnitz*.pp 1025-1029
- [16] Rudenko, A.N. and Mazurenko, V.G. (2007). Calculation of Vibrational Spectra of an Icosahedral Quasicrystal AlCuFe. *ISSN 1063-7745 Crystallography Report*, 5, 10251029.
- [17] FHI-aims (2014)team Fritz-Haber-Institut der Max-Planck-Gesellschaft, Berlin and many
- [18] Ahmad, N., Hasan, A.K. and Keishav, N.S. (2013). DFT calculation of vibrations in the cluster of zinc and oxygen atom. *sains malaysia*, 42(5), 649-654.
- [19] Umrigar, C. (2010). Monte Carlo Methods. *www.physics.cornell.edu/~cyrus*, 32.
- [20] Galadanci,G.S.M.and Babaji, G. (2013). Computations of the Graound State Cohesive Properties of AlAs Crystalline Structure Using Fhi-Aims Code. *IOSR Journal of Applied Physics*, 85-95.
- [21] Hohenberg and Kohn, W. (1964). Inhomogeneous electron gas,. *Phys. Rev.*, 136. B864-871
- [22] Kohn, W. and Sham, L. J. (1965) Self-Consistent equation including exchange and correlation effect. *Physical review* vol. 140 no. 4A pp A1133-1138
- [23] Burke, K. and Friends. (2008). *Basics of DFT*. onlinebooks.
- [24] Martin, R. (2004). *Electronic Structure:Basics Theory and Practical Methods*. Cambridge University Press. *ISBN 785-0-521-78285-2*
- [25] Kratzer, P., Morgan, C.G., Penev, E., Rosa, A.L., Schindlmayr, A., Wang, L.G., and Zywier, T.(1999). FHI98MD Computer Code for Density functional Theory Calculation for Polyatomic Systems: User manual, Program.
- [26] Da Silva, J.L.F., Stampfl, C. and Scheffler, M. (2006). Converged Properties of clean Metal surfaces by All-electron First-Principal Calculation, *Surface science*. 600, 703-715.
- [27] Tkatchenko, A. and Scheffler, M. (2009). *Phys.Rev.Lett*, 102, 6.
- [28] Biswajit S., Angelos M., Martin F., Alexandre T., Claudia F. and Matthias S. (2008). Biswajit S., Ange On the accuracy of density functional theory exchange-correlation function for H. bond in small clusters.II the water hexamer and vander waals interaction. *Journal of Chem.Vol 129* pp194111-12
- [29] Ahlrich R., P. R. (1977). *chem.phy*, 19, 119.

- [30] Wu, Q., and Yang. (2002) Empirical correction to density functional theory for van der Waals interaction. *Journal of chemical physics*. Vol. 116. No 2.
- [31] Grimme, S. (2004). *J.comput.*, 25, 1463.
- [32] Jurecka P., Cerny J., Hobza P. and Salahub D.R. (2007). *J. Comput. Chem.*, 28, 555.
- [33] Blum, V., Gehrke, K., Henk, F., Havu, P., Ren, X., Reuter, K. and Scheffler, M. (2009). *Comput.phys.commun.* 2175.
- [34] Havu, V., Blum, V., Havu, P., and Scheffler, M., (2009). Efficient O(N) integration for all-electron electronic structure calculation using numeric basis function. *J. Comp.Phys.* 8367–8379
- [35] <http://www-wales.ch.cam.ac.uk> retrieve 25th jan 2016